ESI Preprints **Not Peer-reviewed**

Characterization of the vegetation cover and water erosion dynamics in the Aghien lagoon catchment

Ehouman Serge Koffi
Amidou Dao
Dabissi Djibril Noufe
Mamadi Ouedraogo
Nagnon Bernard Yeo
Laboratoire de Géosciences et Environnement,
Université Nangui Abrogoua, Côte d'Ivoire
Luc Seguis
Jean Louis Perrin
IRD, UMR Hydrosciences, Université de Montpellier 2, France
Bamory Kamagate
Lanciné Droh Gone
Laboratoire de Géosciences et Environnement,
Université Nangui Abrogoua, Côte d'Ivoire

Doi: 10.19044/esipreprint.7.2024.p346

Approved: 19 July 2024
Posted: 21 July 2024

Cite As:
Koffi E.S., Dao, A., Noufe, D. D., Ouedraogo, M., Yeo, N. B., Seguis, L., Perrin, J. L., Kamagate, B., & Gone, L. D. (2024). *Characterization of the vegetation cover and water erosion dynamics in the Aghien lagoon catchment*. ESI Preprints.
https://doi.org/10.19044/esipreprint.7.2024.p346

Abstract

Soil erosion affects land quality and water resources. The present research aimed to estimate spatio-temporal changes in land-use/land-cover pattern and soil erosion in the lagoon Aghien watershed in Côte d'Ivoire. This study was carried out by using Landsat imageries of 2016 and 2020. Images were classified into categories using supervised classification by the maximum likelihood algorithm. Universal Soil Loss Equation modeling was applied in a GIS environment to quantify the potential soil erosion risk. The area of bare soil/Habitats and crops/Fallow increased by 2981 ha (37.8%) and 2642 ha (17.58%) during 2016–2020. The high soil losses are located on the slopes of the rivers and valleys adjacent to the Aghien lagoon, which are

also naturally favored by the steepness of the slopes and their length and inclination. However, the average soil loss values were 60.65% in 2016 and 47.64% in 2020. However, the very low and low soil loss values are scattered over the watershed for an area of 34441.52 ha corresponding to a rate of 94.36% in 2016, in 2020 they occupy an area of 34956.76 ha with a rate of 95.77%. On the other hand, high and very high soil losses are insignificant, corresponding to rates of 0.95% and 0.60% in 2016 and 2020 respectively. However, most of the soil loss in the watershed is due to moderate erosion, occupying areas of 1712.19 ha (4.69%) and 1305.77 ha (3.58%) also in 2016 and 2020.

Keywords: Erosion, lagoon Aghien, Abidjan, GIS

1. Introduction

Water erosion is a natural phenomenon that constitutes one of the main factors of soil degradation (Bouguerra et al, 2017). The accentuation of soil degradation depends on several natural and anthropogenic factors favoring the triggering and development of erosion processes. These factors are divided into two categories, those that are quasi-static in nature (infiltration, erodibility and morphology) and others that have variability over time such as vegetation cover, land use, rainfall intensity and agricultural practices (Roose et Lelong, 1976 ; Vrieling, 2005 ; Boukheir et al, 2006 ; Toumi et al, 2013).

In addition, climate change, the influence of population pressure (Mazouzi et al, 2021) and the extension of cash crops have contributed to an increase in the exposure of land to the runoff process, and consequently to soil degradation through erosion (Das et al, 2020). Various kinds of human activities, agricultural practices, forestry, grazing, road construction (Belaout et al, 2021) and buildings tend to modify erosion phenomena, often accelerating it considerably (Wachal et al, 2009). It results from the detachment, under the effect of the kinetic energy of raindrops, and the transport of fragments or particles, (Kinnell, 2016; Benchettouh et al, 2021) of soil or rock from their initial location by water, degrading water quality and soil fertility and considerably reducing the capacity of reservoirs, but also siltation of hydro-agricultural infrastructures (Kouassi et al, 2020 ; Khemiri and Jebari 2021). The significant impacts of soil erosion include poor soil productivity, degraded water quality due to eutrophication in water bodies, siltation, and sedimentation of lakes and river beds, enhances Cood risk, etc. (Onyando et al, 2005 ; Zhou et al, 2008 ; Das et al, 2020).

In Côte d'Ivoire, the first works on land erosion are those of Rougerie (1958 and 1960), carried out in the forest region, which made it possible to analyze the various erosion processes, factors and anti-erosion methods.

Several studies on water erosion have been carried out in Côte d'Ivoire, including those on the coast (Adopo et al, 2014; Abé et al, 2014) and Coulibaly et al, (2021) carried out their study on the Boubo coastal watershed. Other authors have focused their studies in certain regions of the country such as Bonoua (Aké et al, 2012), Adiaké (Eblin et al, 2017), Korhogo (Koukougnon et al, 2021), Man (Kouadio et al, 2007). Some studies have focused on the watershed such as the Lake Buyo watershed (Koua et al, 2019), the Mé River (Kouadio et al, 2018), the Lobo River (Déguy et al, 2018), in the watershed of the hydro-agricultural dam of Babadou (Kouassi et al, 2020). N'Dri et al, (2017) conducted their investigation in the autonomous district of Abidjan, precisely in the commune of Attécoubé, on experimental plots. These authors showed that erosion leads to significant modifications of natural environments.

The increase in the population of the Autonomous District of Abidjan in recent years as a result of the socio-political crisis and waves of migration of people from the interior of the country and neighboring countries (Nana, 2018) has led to a high demand for housing. This demand has led to a wave of real estate construction owned by property developers with the aim of housing all this population. These constructions are first followed by major earthworks, thus contributing to the degradation of the vegetation cover. The soil, once stripped of its vegetation cover, suffers the consequences of the climate.

The present work uses the USLE model coupled with a Geographic Information System (GIS). This approach makes it possible to estimate water erosion and its spatial distribution in large areas, on the scale of the watershed and the country, or even the continent (Khemiri and Jebari, 2021).

The objective of this manuscript is to analyze and spatialize the different factors involved in the erosion phenomenon in order to elaborate the thematic map of erosion risks and soil losses in the Aghien lagoon catchment area. The identification of vulnerable areas from the soil loss map will enable decision makers to take measures for the protection and efficient management of the Aghien Lagoon.

2. Material and methods

2.1. Study Area

The Aghien lagoon watershed is located in the North-East of Côte d'Ivoire (Diallo et al. 2018), on the outskirts of the autonomous district of Abidjan between longitudes 375,000 m and 410,000 m West and latitudes 598,000 m and 619,000 m North. It is a peri-urban basin straddling three (03) communes of the district. It is urbanized, encompassing the most populated districts of the commune of Abobo. Its surface area is 365 km². It associates in particular 2 basins drained by the Djibi and Bété rivers, tributaries of the

Aghien lagoon. The Bété basin has an area of 216 km² and the Djibi basin covers 78 km² (Diallo et al. 2018).

The distribution of the climate is regulated by the seasonal displacement of air masses that sweep through the south-eastern region. Very dry tropical continental air descends from the Sahara in a north-south direction (harmattan), while humid maritime equatorial air, called monsoon, is fed by the St Helena high. The ballet between these two air masses regulates the climate where the study area is located and subdivides it into four major seasons that mark the hydrological cycle. The by bi-modal rainy seasons (May–July and October–November), separated by two dry periods (July–September and December–April) (Koffi et al. 2019).

The sedimentary basin in which a large part of the Aghien lagoon's catchment area is located is a large, flattened crescent, bordering the Atlantic coast from Sassandra to Ghana. It extends over 45 km inland and does not exceed 130 m in altitude with a surface area of 8,000 km². The sedimentary basin is of Cretaceous-Quaternary, Meso-Cenozoic and Paleoproterozoic age. It is mainly composed of clayey sands and coastal sands. It is crossed from west to east by the major accident of the lagoon fault with a rejection of nearly 3,000 m (Kouassi, 2013; Traoré, 2016).

It has Quaternary sands and muds on the eastern edge of the Aghien lagoon. Continental Terminal (Tertiary) sands, clays and ferruginous sandstones are the most abundant.

The slopes of the Aghien catchment area are between 0 and 20° with an average of 4° and a standard deviation of 2.8°. They are generally low. The low slopes are located in the alluvial zones of the main tributaries, upstream of the catchment area and in the urban areas on the plateaus upstream of the Djibi. Steep slopes are found at the edges of the plateau incisions with steep slopes oriented towards the lagoon (Koffi et al, 2019).

The vegetation in the study area is characterized by evergreen forest. This woody formation is composed by the presence of large trees, some of which are sought after. Unfortunately, this forest has suffered a strong regression due to anthropic activities and is now replaced by a mosaic of classified forests.

The vegetation on the borders of the Aghien lagoon is mainly dominated by swamp forest composed of mangroves and bamboos. This vegetation plays an important role in the stability of the lagoon environment. It acts as a buffer zone by preventing nutrients and sediments from being discharged into the Aghien lagoon and ensures wildlife habitat (N'Dri et al. 2017).

The average monthly temperature varies between 24.7°C and 27.8°C. Higher temperatures are observed from February to April during the long dry

season. The onset of the main rainy season with the appearance of clouds leads to a drop in temperature, the lowest being in August (24.77°C).

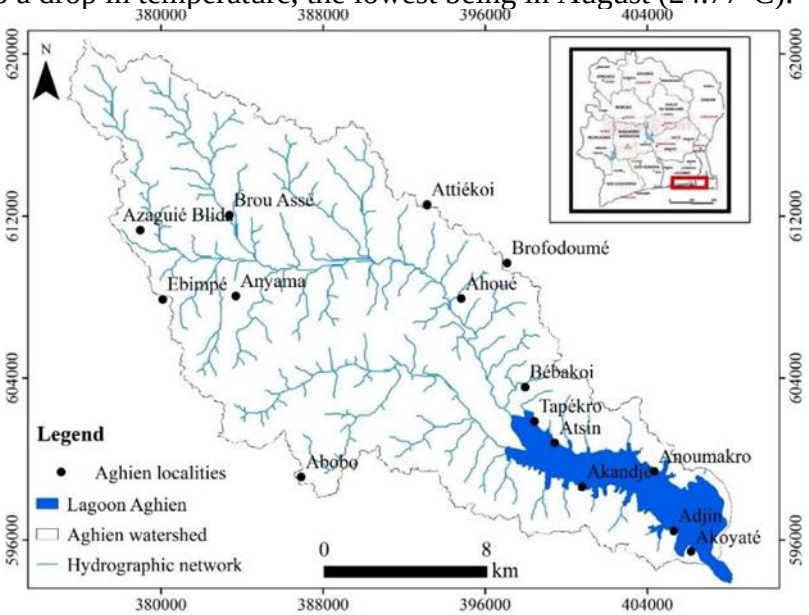

Figure 1 : Location of lagoon Aghien watershed

2.2. Data used

The annual rainfall for 2016 and 2020 was calculated from rainfall data collected at rainfall stations installed in the Aghien lagoon catchment since 2015.

The distribution of R values was assumed to vary consistently with annual precipitation across the watershed. The highest value of the annual R factor was observed between

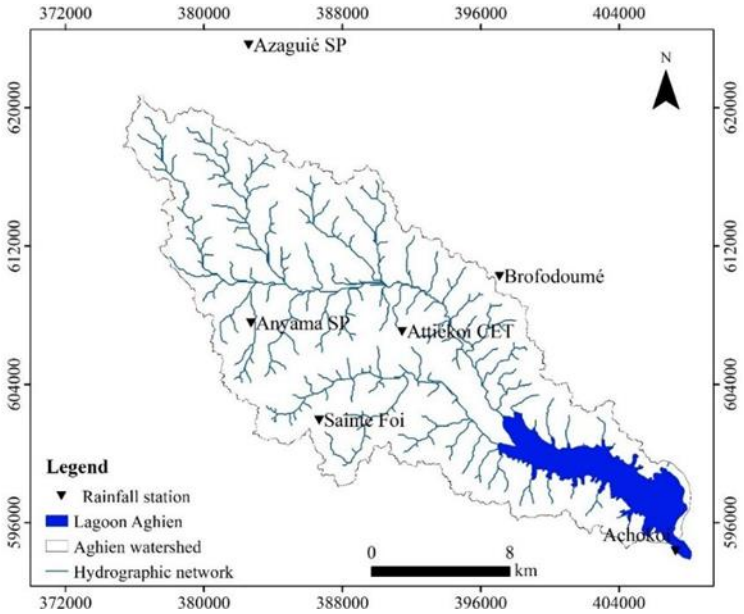

Figure 2 : Rainfall station in the watershed of the Aghien lagoon

The **Figure 3** shows the annual rainfall values by station; the 2016 rainfall is above 2400 mm (Anyama, Attiékoi CET, Achokoi, Brofodoumé and Sainte Foi), except at the Azaguié station where the rainfall is below 2000 mm (1900 mm). However, the rainfall for the year 2020 is slightly above 2000 mm, and these values are observed at the stations of Achokoi in the commune of Bingerville, Anyama and Sainte Foi in the commune of Abobo. As for the Azaguié, Brofodoumé and Attiékoi CET stations located in the periphery of the autonomous district of Abidjan, the rainfall is less than 2000 mm. Generally speaking, rainfall in 2016 was higher than in 2020

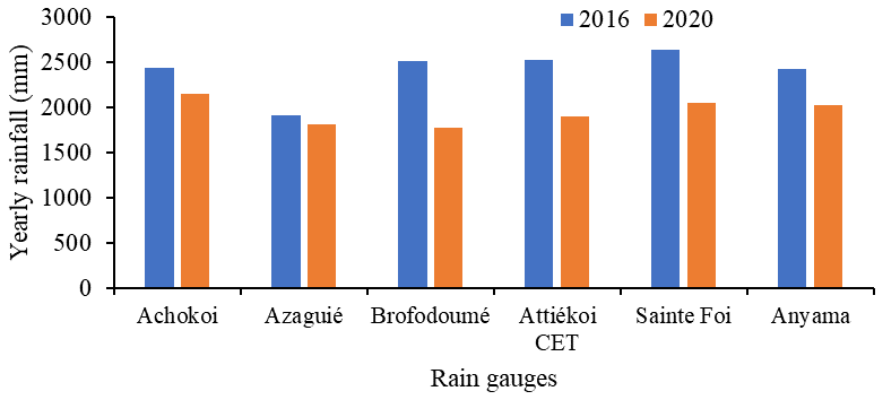

Figure 3 : Pluie annuelle des stations pluviométriques du bassin versant de la lagune Aghien

Satellite images from Landsat 8 (OLI) for 2016 and 2020 were downloaded from the Nasa website (https://earthexplorer.usgs.gov) at 30 m WGS 84 resolutions. Landsat 8 band designations for the Operational Land Imager (OLI).

Table 1 : The resolution of the images is recorded in the table

Band Number	Description	Wavelength (µm)	Resolution
Band 1	Coastal / Aerosol	0.433 to 0.453	30
Band 2	Visible blue	0.450 to 0.515	30
Band 3	Visible green	0.525 to 0.600	30
Band 4	Visible red	0.630 to 0.680	30
Band 5	Near-infrared	0.845 to 0.885	30
Band 6	Short wavelength infrared	1.56 to 1.66	30
Band 7	Short wavelength infrared	2.10 to 2.30	30
Band 8	Panchromatic	0.50 to 0.68	30
Band 9	Cirrus	1.36 to 1.39	30
Band 10	Long wavelength infrared	10.3 to 11.3	100
Band 11	Long wavelength infrared	11.5 to 12.5	100

Table 2 : Satellite images used

Acquisition data	Sensor	Path/row
05/01/2016		
28/01/2016	Landsat 8 OLI/TIRS	196-56 and 55
07/01/2020		

2.3. Land use change rate

The different vegetation classes or land cover were mapped from the supervised classification of a LANDSAT 8 ORLI multispectral satellite image. It was first pre-processed, corrected, combined and masked. After the creation of ROI areas on the image, a supervised classification of maximum likelihood type was then carried out. This method calculates, according to the reflectance of the pixels, the probability of their belonging to a given class. A validation step of the result by the confusion matrix finally allowed to obtain a map of the vegetation cover with five classes.

The rate of change of land cover classes was used to express the variation of land cover between two dates. According to Diallo et al, (2018), this rate was calculated by the following relationship

$$T = \frac{V_f - V_i}{V_f}$$

Where T: Rate of change of vegetation cover between the two dates of dates;
Vi: The proportion of the land cover class taken at the initial state;
Vf: The proportion of the land cover class taken at the final state.

2.4. Generation of the thematic maps of RUSLE model

The USLE is an empirical soil model developed by Wischmeier and Smith, (1978). Originally, USLE was developed mainly for soil erosion estimation in croplands or gently sloping topography (Ganasri and Ramesh, 2016). The USLE quantifies soil erosion as the product of five factors representing rainfall and runoff erosivity (R), soil erodibility (K), slope length (L), slope steepness (S), cover and management practices (C), and supporting conservation practices (P) (Renard and Freimund, 1994 ; Panagos et al. 2015a et 2015b ; Benchettouh et al. 2021 ; Piyathilake et al. 2020 ; Khemiri and Jebari, 2021 ; Payet et al. 2012).

This empirical equation is based on the statistical analysis of more than 10,000 plot-years of data of sheet and rill erosion on plots and small watersheds (Roose, 1977). The equation is:

$$A = R * K * C * LS * P$$

Where: A: expresses the average annual land loss (t/ha/year), R: rainfall aggressiveness (MJ.mm/ha/hr/year), K: represents the soil erodibility factor (t/ha/MJ/mm/ ha.h), LS: topographical factor (L = slope length factor and S= slope steepness factor), C: corresponds to the cultivation (vegetation) and management factor, dimensionless, P: corresponds to the conservation practice factor, dimensionless.

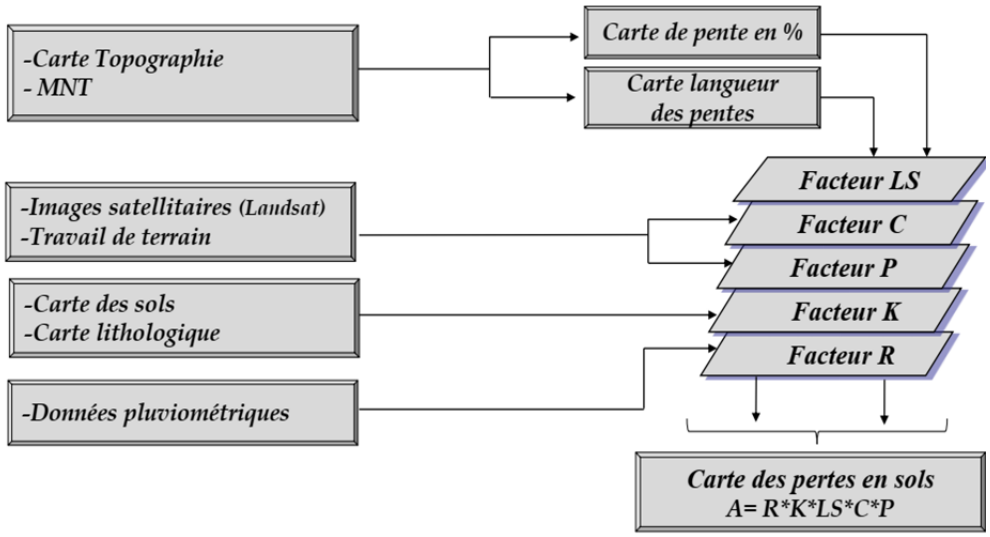

Figure 4 : Methodology for estimating soil loss (Meliho et al. 2016)

2.4.1. Support practice factor (P)

The P factor is the ratio of soil loss from a land with given support practice to the corresponding loss from an experimental plot having an agricultural practice of upslope and downslope tillage (Swarnkar et al. 2018). Also, the anti-erosion practices are contour cultivation, alternate strip or

terrace cultivation, bench reforestation, ridging (Table 3). P values range from 0 to 1, where 0 represents a very good environment for resistance to human-induced erosion and 1 shows no anti-erosion practice (El Garouani et al. 2008). The methodology is summarized in Figure 5 .

Table 3 : Correspondence between slopes and the different types of crops recommended by Shin (1999)

Slope (%)	Crops in contour	Crops in band	Terrace with contour crops
0.0 – 7.0	0.55	0.27	0.10
7.0 – 11.3	0.60	0.30	0.12
11.3 – 17.6	0.80	0.40	0.16
17.6 – 26.8	0.90	0.45	0.18
26.8 >	1.00	0.50	0.20

Figure 5 : Steps for mapping the P factor under [43] Shin (1999)

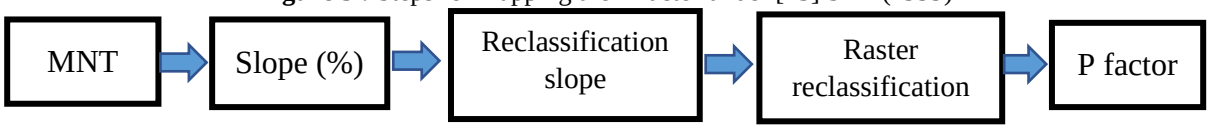

2.4.2 Rainfall-runoff erosivity factor (R)

Table 4 : Rainfall erosivity (R) values

	2016 Rainfall (mm)	R (MJ mm ha^{-1} h^{-1} $year^{-1}$)	2020 Rainfall (mm)	R (MJ mm ha^{-1} h^{-1} $year^{-1}$)
Achokoi	2437.30	1462.38	2150.5	1290.3
Azaguié	1909.00	1145.40	1818.2	1090.92
Brofodoumé	2509.80	1505.88	1780	1068
Attiékoi CET	2527.30	1516.38	1907	1144.2
Sainte Foi	2638.50	1583.10	2050	1230
Anyama	2425.70	1455.42	2024.3	1214.58

The R factor depends on rainfall–runoff characteristics, which are in turn influenced by geographic location. Therefore, the rainfall characteristics of the entire watershed (36500 ha) were considered to be adequately represented by data collected from the six-weather station in the study area. Rainfall data were collected from six meteorological station within the study watershed from 2016 to 2020. Rainfall–runoff erosivity was determined by Roose (1977, 1985) method (P: annual rainfall).

$$R = P * 0.6$$

The altitude map, derived from the 30 m DTM (**Figure 6**), shows that the altitudes vary between 0 m and 137 m in the Aghien catchment area. The

highest altitudes are found in the commune of Abobo and in the northern periphery of the catchment area. These altitudes more or less form the water divide. The low levels are located towards the south of the catchment area. These low areas are more or less homogeneous and are located to the south-east of the Aghien lagoon watershed.

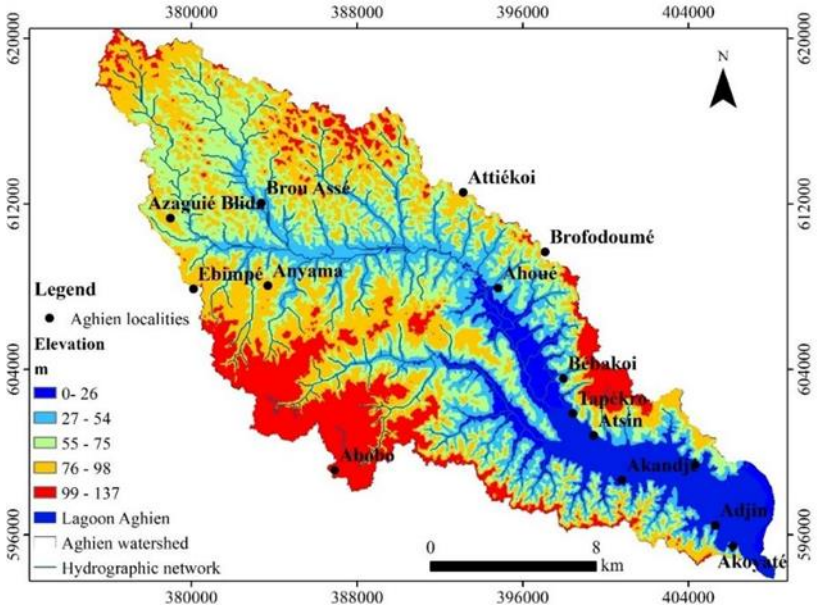

Figure 6 : Elevation class map of lagoon Aghien watershed

2.4.3. Soil erodibility factor (K)

Erodibility is the rate of erosion due solely to the inherent properties of the soil itself. The K-factor expresses the susceptibility of soil erodibility to resist erosion due to rainfall and runoff (Anache et al. 2015 ; Songu et al. 2021). The K-factor is a measure of the vulnerability of soil particles to detachment and transport by rainfall and runoff. Texture is the main factor influencing the K-factor, but soil structure, organic matter content and permeability also play a role (Stone and Hilborn, 2000; El Garouani et al. 2008; Markhi, 2015).

Table 5 : General sensitivity of soil texture to erosion [47] (Stone and Hilborn 2000)

Area soil class	Relative sensitivity to water erosion	OM content			Correspondence of the soils in the Aghien watershed
		< 2 %	> 2 %	Average.	
Very fine sand	Very high	0.46	0.37	0.43	
Very fine loamy sand	High	0.44	0.25	0.39	
Silty loam		0.41	0.37	0.38	
Very fine sandy loam		0.41	0.33	0.35	
Silt-clay loam		0.35	0.30	0.32	
Clay Loam		0.33	0.28	0.30	
Loam		0.34	0.26	0.30	
Silty clay	Moderate	0.27	0.26	**0.26**	Ferrallitic sandy-clay soil
Clay		0.24	0.21	**0.22**	Hydromorphic soil
Sandy clay loam		–	0.20	0.20	
Heavy clay		0.19	0.15	0.17	
Loamy sand		0.05	0.04	**0.04**	Ferrallitic sandy-clay soil
Fine loamy sand	Slight	0.15	0.09	**0.11**	Complex ferrallitic soil
Fine sand		0.09	0.06	0.08	
Coarse sandy loam		–	0.07	**0.07**	Sandy ferrallitic soil
Sandy loam	Very lignt	0.14	0.12	0.13	
Sand		0.03	0.01	0.02	

2.4.4. Cover-management factor (C)

Soil that is well protected by vegetation cover greatly reduces the effects of climatic aggressiveness, soil erodibility, and slope gradient, regardless of their importance in the sense that appropriate cover facilitates infiltration, thus reducing runoff and preventing the onset of erosion (Meliho et al. 2020).

The C factor reflects the effect of cropping and management practices on soil erosion rates in agricultural lands and the effects of vegetation canopy and ground covers on reducing soil erosion in forested regions (Renard et al,

1996 ; Meliho et al. 2020). In recent years, because of large spatial and temporal variability of vegetation cover, satellite images have been used to extract the factor C (Karydas et al, 2009; Tian et al, 2009).

The C-factor expresses the weighted ratio of soil losses over a land use situation to those measured in a unit plot (Renard et al. 1996 ; Batista et al. 2017). Therefore, it reflects not only land use, but also crop type, tillage practices and other conservation conditions (Panagos et al. 2015a). Values of the C-factor range from 0 to 1.0, with lower values corresponding to densely vegetated landscapes, such as forested areas, and higher values corresponding to bare soil.

For catchment scale erosion modelling, C-factor values can be assigned to land use classes (Panagos et al. 2015a and 2015b). In this study, land cover maps were produced using Landsat 8 Surface Reflectance images of 30 m resolution, dated 2016 and 2020. A supervised classification was performed to obtain the cover classes (Trimble, 2010). Finally, C-factor values were assigned to the identified land use classes (Table 6).

Table 6 : Land use coefficient C as a function of land use type [38] (Payet et al, 2012)

Type of land use	C Factor
Bare soil	1
Degraded forest	0.7
Savannah with trees and shrubs	0.3
Degraded Grass Savannah	0.6
Mosaic of culture	0.5
Mangrove	0.28
Habitats	0.2
Wooded area	0.18
Paddy field	0.15
Dense forest	0.001
Water bodies	0

2.4.5. Topographic factor (LS)

Topography is one of the main factors in soil erosion and hydrological modeling, because it defines the effect of gravity on the movement and flow of water and sediments. The length (L) and steepness of the slope (S) affect sediment yield (Meliho et al. 2020).

The topographic factor (LS) depends on both the slope length (L) and the slope steepness (S). Erosion increases with the length and inclination of the slopes (Bollinne and Rosseau, 1978; Bollinne and Laurant, 1983). The calculation of the LS-factor of the Aghien lagoon is carried out on a GIS-support. The latter uses the DEM (Digital Elevation Model) to calculate the slope in degrees, the orientation and the cumulative length. The combination of the L and S factor gives the LS factor. The LS-factor is a ratio of the soil loss under given conditions to the soil loss at a location with a "standard"

slope of 9% and a slope length of 22.1 m. The steeper and longer the slope, the higher the erosion risk (Wischmeier and Smith, 1978). The formula used was developed by Desmet and Govers (1996). Topography plays a significant role in erosion or landslide. The topographic factor (LS) depicts the effects of topography on erosion and contains the length and steepness of the slope that influence the surface runoff speed (Biswas and Pani, 2015).

$$L = ((A + D^2)^{m+1} - A^{(m+1)})/(X^m D^{(m+2)} * 22.1^m \quad (1)$$

Where A (m) is the area at the input of a pixel (cell), D is the pixel size and x is the shape correction factor.

$$m = \frac{F}{F+1} \quad (2)$$

$$F = \left(\frac{\frac{sinsin("slope"*0.01745)}{0.0896}}{3*power(sinsin("slope"*0.01745),0.8)+0.56}\right) \quad (3)$$

$$S = 10.8 * sin\theta + 0.03 \; for \; slope < 9\% \quad (4)$$

$$S = 16.8 * sin\theta - 0.05 \; for \; slope \quad (5)$$

The slopes of the Aghien catchment area range from 0 to 35.5° with an average of 6.2° and a standard deviation of 4.7°. The slopes are generally low. The very low and low slopes occupy 95.95% of the surface area of the Aghien catchment area and are located in the alluvial zones of the main tributaries, in the upstream part of the catchment area and in the urban areas on the plateaus of the Djibi River. On the other hand, steep slopes are found at the edges of the plateau incisions facing the lagoon (Koffi et al. 2014), and are also found on the slopes of the Bété and Djibi rivers. steep and very steep slopes occupy 0.22% of the study area (Table 6 et Figure 7).

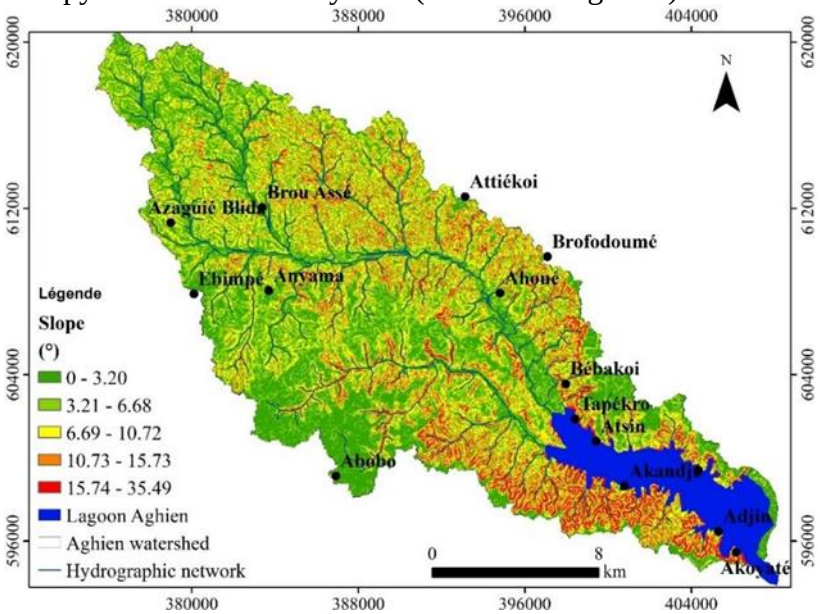

Figure 7 : Slope map of lagoon Aghien watershed

Table 7 : Declivity classes

Slope (°)	Area (ha)	Area (%)	
0-3.20	25922,32	71,02	Very low
3.21-6.68	9097,63	24,93	Low
6.69-10.72	1400,49	3,84	Moderate
10.73-15.73	76,31	0,21	High
15.74-35.49	3,25	0,01	Very high

3. Results and discussion

3.1. Land use

The land use map (**Figure 8** A and B) was prepared on the basis of land use cover map of the study areas. The land use is classified with five main classes, namely, water body, forest area, degraded forest, crops/fallow, bare soil.

The watershed of the Aghien lagoon was dominated in 2016 by degraded forest and crops and fallow land (Figure 8 A) with respective surfaces of 16011 and 12384 ha for proportions of 44.81% and 33.92% of the total area of this watershed. In 2017, the area of the degraded forest class decreased to 11122 ha (30.4%), i.e. a reduction of 4889 ha. This entity was replaced by crops and fallow land, which grew to 15026 ha (41.15%), an increase of 2642 ha. This regression was also in favour of habitat, which increased from 4906 ha in 2016 to 7887 ha in 2017 over the entire watershed (**Table 8**). Bare soil and habitats are concentrated in the south of the watershed, dominated by the communes of Anyama and Abobo. The few forests present in the study area are pockets of classified forest that are gradually being destroyed in favour of industrial crops and the expansion of the autonomous district of Abidjan. The area of forest, which was 1253 ha (3.43%) in 2016, fell to 540 ha (1.48%) in 2017, a decrease of 713 ha. The surface area of the lagoon water body underwent a very slight variation from 1957 ha in 2016 to 1936 ha in 2017.

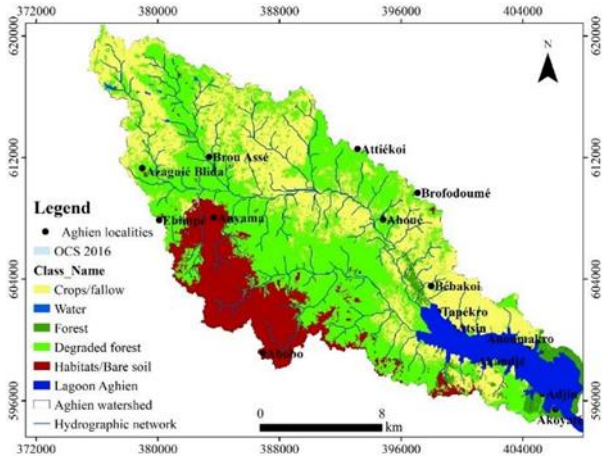

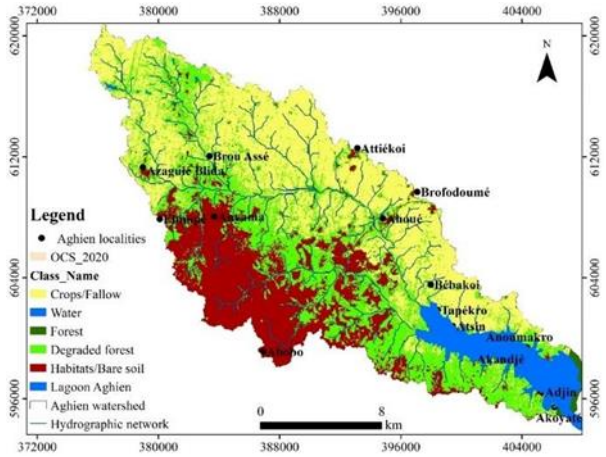

Figure 8 : Land use/land cover in lagoon Aghien watershed. A : 2016 ; B : 2020

Table 8 : Land use class

	2016		2020		2016-2020	
					Area change (ha)	Area change (%)
Class name	Area (ha)	Area (%)	Area (ha)	Area (%)		
Soil bare/Habitat	4906	13.44	7887	21.60	2981	37.80
Forest	1253	3.43	540	1.48	-713	-132.04
Water	1957	5.36	1936	5.3	-21	-1.08
Crops/Fallow	12384	33.92	15026	41.15	2642	17.58
Forest degraded	16011	43.85	11122	30.46	-4889	-43.96

3.2. USLE factor mapping

3.4.1. Rainfall erosivity factor (R)

The average annual rainfall erosivity factor (R) for six weather stations was found to be in the range of 1145 and 1583 MJ mm ha^{-1} h^{-1} $year^{-1}$, in 2016 1068 and 1290 MJ mm ha^{-1} h^{-1} $year^{-1}$ in 2020 (**Table 4 ; Figure 9** A and B). With an average 1478 and 1175 MJ mm ha^{-1} h^{-1} $year^{-1}$ respectively in 2016 and 2020 (**Table 9**).

The thematic maps of the R-factor have been grouped into five categories starting from very low, low, moderate, high and very high classes. This classification was performed for all thematic maps of the USLE.

The spatial distribution of the year 2016 shows that the lowest and weakest values of erosivity are confined to the north of the catchment area precisely in the Brou Assé region. On the other hand, the highest values are grouped in the center of the catchment area, while the high erosivity is

located on both sides of the high erosivities. The moderate values are framed by the low and high erosivity values (**Figure 9**).

In contrast, the spatial distribution for the year 2020 reveals a map cut off from high and very high erosivity (**Table 9; Figure 9**B). The catchment area is largely covered by very low erosivity in the north in the village of Ahoué, Attiékoi, etc.; low erosivity in the south in the commune of Abobo, Anyama, etc. Moderate erosivity is located to the east of the Aghien lagoon watershed.

This spatial distribution shows once again the heterogeneous character of erosivity and could also be a function of the variability of rainfall collected at the rainfall stations

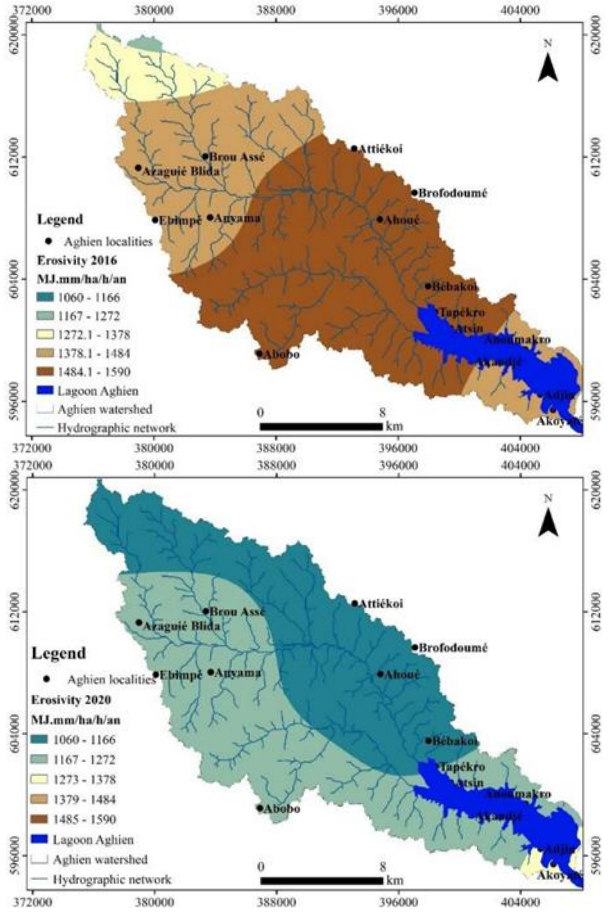

Figure 9 : Spatial distribution of the R factor in lagoon Aghien watershed. A : 2016 ; B : 2020

Table 9 : R-factor distribution in lagoon Aghien watershed

	2016			2020		
R factor (MJ.mm/ha/h/an)	**Area (ha)**	**Area (%)**	**Average (MJ.mm/ha/h/an)**	**Area (ha)**	**Area (%)**	**Average (MJ.mm/ha/h/an)**
1066 - 1166	0.09	0.00		15746.13	43.14	
1167 - 1272	196.72	0.54		19886.37	54.48	
1273 - 1378	2459.70	6.74	1478.1	867.50	2.38	1175.6
1379 - 1484	13280.02	36.38				
1485 - 1590	20563.47	56.34				

3.4.2. Topographic factor (LS)

The values of the LS factor vary between 0 and 15, where the very low and low class (0 - 3.18) occupies the most dominant area of the catchment with 81.65 %. The average LS value between 3.19 and 5.68 occupies the 15.35% of the Aghien lagoon catchment area. The high and very high LS values (5.69 - 225) are present in only 3.05 % of the catchment area. These results are proportional to the topography of the basin, which is dominated by relatively flat areas scattered over the basin where low slopes are observed in 85.95% (less than 10° slope (**Table 7**)). The high and very high values of LS are attributed to the downstream part of the basin where the relief is high and to the areas close to the main slopes of the Bété and Djibi rivers. The average LS value is 1.84 (**Table 10; Figure 10**).

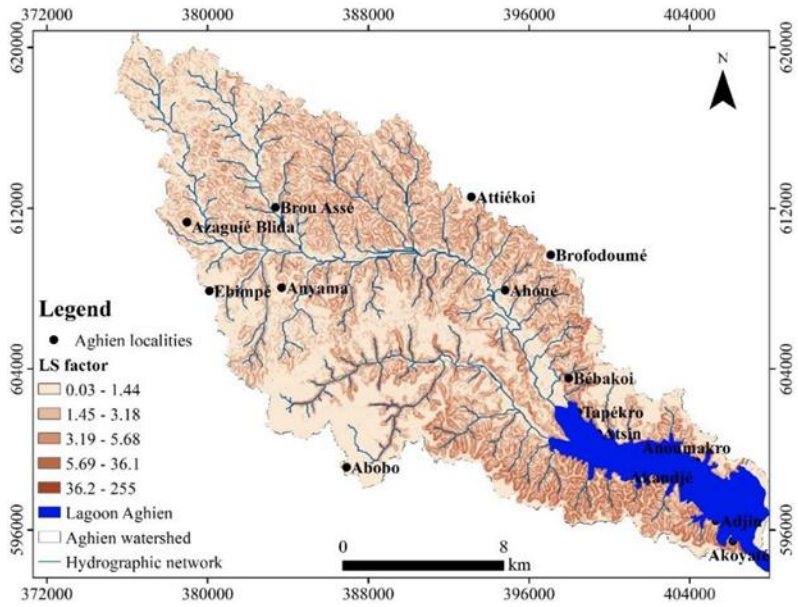

Figure 10 : Spatial distribution of the LS Factor in lagoon Aghien watershed

Table 10 : Topographic factor

LS Factor	Area (ha)	Area (%)	Average
0.03-1.44	19891.7092	54.53	1.84
1.45-3.18	9876.65	27.08	
3.19-5.68	5600.41079	15.35	
5.69-36.10	1103.72266	3.03	
36.11-255	6.11952051	0.02	

3.4.3. Soil erodibility K-factor

The calculated K-factor in the Aghien lagoon catchment area varies from less than 0 to 0.26 t/ha/MJ/mm and has an average value of 0.13 t/ha/MJ/mm, which is relatively high (**Figure 11** ; **Table 11**).

The lowest and low values are mainly located in the northern part and around the basin, occupying 30.66% of the basin area. The high to very high values are located in the marl-clay soils, covering 24.53% of the basin area. The modest K values take up most of the Aghien lagoon catchment area. These areas represent 44.81% of the catchment area.

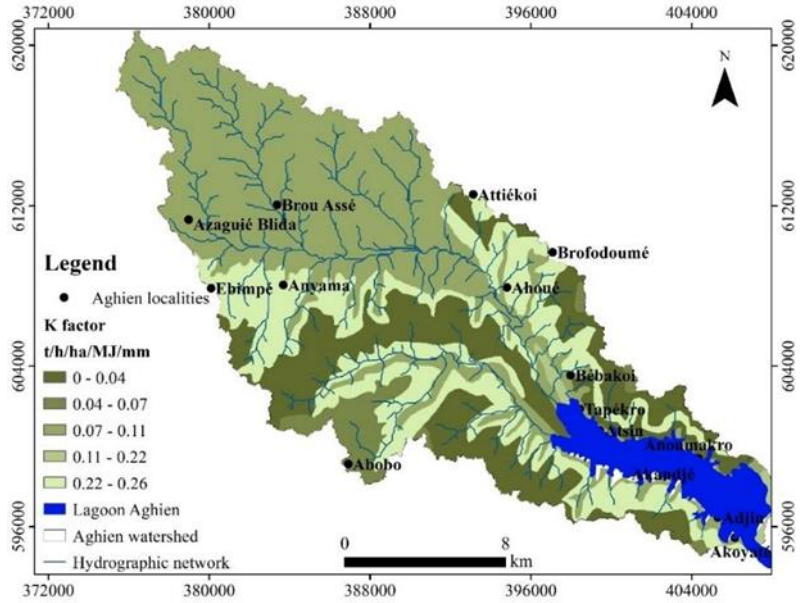

Figure 11 : Spatial distribution of the K Factor in lagoon Aghien watershed

Table 11 : Soil types and their K values in lagoon Aghien watershed

K factor (t/ha/MJ/mm)	Area (ha)	Area (%)	Average (t/ha/MJ/mm)	Soil type
0-0.04	9799.53	26.85	0.13	Ferrallitic sandy-clay soil
0.05-0.07	1391.58	3.81		Ferrallitic sandy soil
0.08-0.11	16356.36	44.81		Complex ferrallitic soil
0.18-0.22	350.88	0.96		hydromorph soil
0.23-0.26	8601.79	23.57		Ferrallitic sandy-clay soil

3.4.3. Crop management factor (C)

The values of the C-factor, scaled to the same level for the purpose of comparing the 2016 and 2020 maps, vary between 0.02 and 1, having respective averages of 0.61 and 0.63 as shown in **Table 12** and **Figure 12** A and B. The map shows that the lowest values are associated with the lower elevations. The major part of the studied catchment area has high and very high values of the C-factor ranging from 0.6 to 1, covering 54.16 and 51.95% of the catchment area in 2016 and 2020 respectively, and are related to bare soil, housing expansion and market gardening. The spatial distribution of factor C shows that the study area is undergoing anthropisation due to human activities. Land use and rainfall variability have led to the degradation of forests by transforming these areas into cultivated land. The results from factor C show that 8.78% (2016) and 6.73% (2020) of the basin area has very low vegetation cover. Areas with low vegetation cover are highly susceptible to water erosion. Moderate values of the C-factor in the range (0.4 - 0.6) for proportions of 34.05% in 2016 and 41.31% in 2020 occupy the northern areas of the catchment.

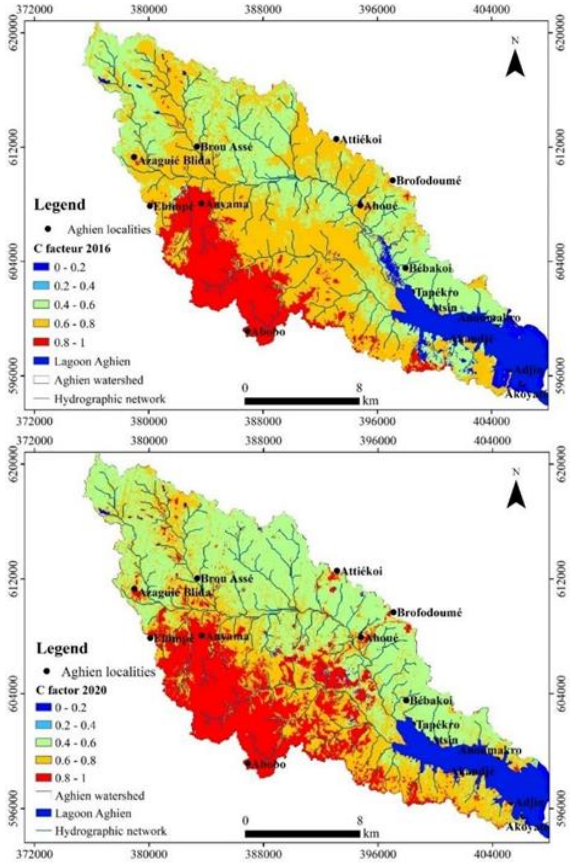

Figure 12 : Spatial distribution of the C factor in lagoon Aghien watershed. A : 2016 ; B : 2020

Table 12: C factor temporal evolution in lagoon Aghien watershed

	2016			2020		
C factor	**Area (ha)**	**Area (%)**	**Average**	**Area (ha)**	**Area (%)**	**Average**
0 – 0.2	3206.61	8.78	0.61	2457.09	6.73	0.63
0.2 – 0.4						
0.4 – 0.6	12431.87	34.05		15081.79	41.31	
0.6 – 0.8	15980.22	43.77		11022.72	30.19	
0.8 - 1	4888.47	13.39		7945.42	21.76	

3.4.4. Conservation Practice (P) Factor

The value of the (dimensionless) P-factor ranges from 0 to 0.55 with an average of 0.29. This study showed that 86.96% of the Aghien Lagoon catchment area had a P-factor between 0 and 0.3, representing very low to low values of the P-factor. Topographical features can affect erosion. The lower the P value, the more effective the conservation practice is considered to be in reducing soil erosion. The high and very high P-values occupy 1.58% of the catchment area. This corresponds to the steepest slopes. The P-factor map was developed from the slope map. These values are concentrated in the Aghien lagoon.

The map shows that the value of the P-factor is associated with the topographical features and the value is high in the whole catchment area (**Figure 13** ; **Table 13**).

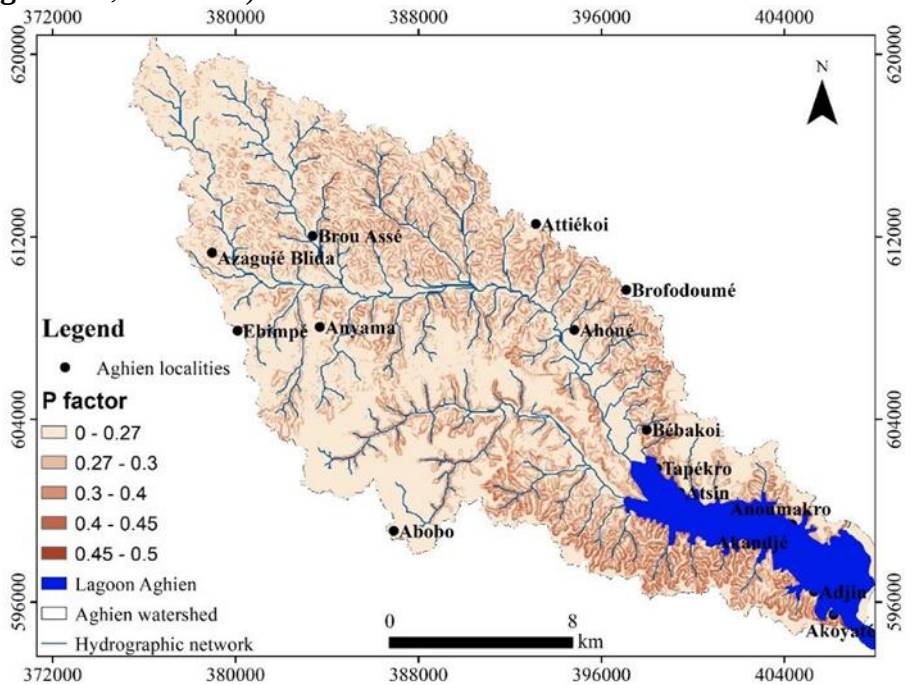

Figure 13 : Spatial distribution of the P Factor in lagoon Aghien watershed

Table 13 : Conservation practice factor (P) values in lagoon Aghien watershed

P factor	Area (ha)	Area (%)	Average
0-0.27	24550.27	67.26	0.29
0.28-0.3	7190.10	19.70	
0.31-0.4	4037.17	11.06	
0.41-0.45	711.62	1.95	
0.46-0.5	10.83	0.03	

3.4.6. Soil loss

The USLE layers derived for R, K, LS, C and P factors were integrated within the raster calculator option of the ArcGIS ver. 10.2 spatial analyst in order to quantify and generate soil erosion risk and severity maps for the lagoon Aghien watershed. The influence of environmental factors on spatial distribution of soil erosion loss (terrain units, elevation, slope, and land use/cover) were analyzed and evaluated.

The soil loss map produced has been grouped into five categories which are: the very low and low class, the moderate class and the high and very high class. The soil loss map for the year 2016 has been set to the same as the one for 2020 for a better comparison. The soil loss varies between 0 and 9230 t/ha/year, with an average of 60.65 t/ha/year in 2016 and 47.64 t/ha/year in 2020 (**Figure 14** A and B). The very low to low categories are prevalent over almost the entire area of the basin. They occupy 94.36% of the catchment in 2016 and 95.77% in 2020 (**Table 14**). This class is scattered over the basin, in both low-lying and high-lying areas. A slight increase of 1.47% is observed from 2016 to 2020. On the other hand, the high and very high classes cumulate 0.95% and 0.65% respectively in 2016 and 2020, a decrease of 46.15% is observed. The moderate class occupies 4.69% of the area of the 2016 basin and 3.58% of the area of the 2020 basin. This class is located on the slopes of the watercourses and steep slopes along the Aghien lagoon.

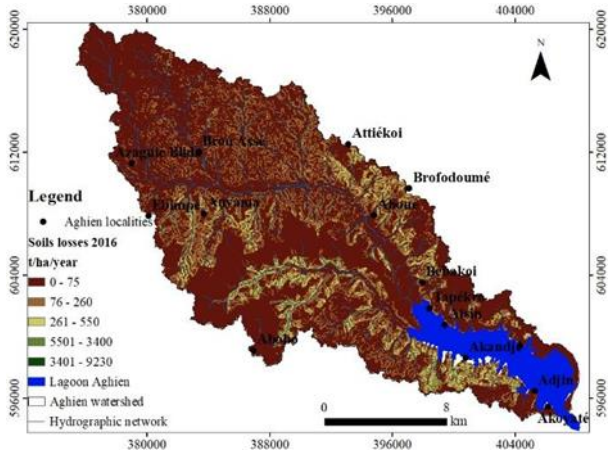

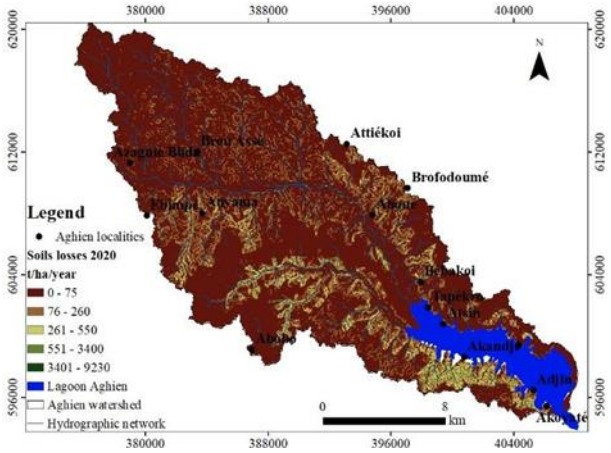

Figure 14 : Spatial distribution of soil losses in lagoon Aghien watershed. A : 2016 ; B : 2020

Table 14 : Soil loss and erosion risk classes of the watershed

Soil loss (t/ha/year)	2016			2020			Erosion class
	Area (ha)	Area (%)	Average (t/ha/year)	Area (ha)	Area (%)	Average (t/ha/year)	
0-75	26095.03	71.49	60.65	28244	77.38	47.64	Very low
76-260	8346.49	22.87		6712.76	18.39		Low
261-550	1712.19	4.69		1305.77	3.58		Moderate
551-3400	345.69	0.95		237.36	0.65		High
3401-9230	0.61	0		0.10	0		Very high

3. Discussion

Soil loss maps from the USLE method (Wischmeier and Smith, 1978), derived from the combination of the factors R, K, LS, C and P, were integrated into the raster calculator option of the spatial analyzer ArcGIS ver. 10.2 in order to quantify and generate thematic soil erosion risk and severity maps for the watershed of the Aghien lagoon. The R-factor representing the aggressiveness of precipitation is higher in 2016 than in 2020, these high values could be attributed to the high annual precipitation (Almaaitah et al. 2018) recorded and ranging from 1909 to 2638 mm of the instantaneous cumulative values collected at the different rainfall stations installed in the Aghien lagoon watershed. This rainfall follows a decreasing gradient from south to north towards the high altitudes (Khanchoula et al. 2020; Meliho et al. 2020). However, the vegetation cover plays an important role in soil protection (Koua et al. 2019; Kilic, 2021), and a soil without vegetation cover can be affected by rain (Coulibaly et al. 2021). Indeed, the kinetic energy of a raindrop is transformed on impact into mechanical energy capable of moving soil particles, even on a very gentle slope (Eblin et al. 2017). Under the effect of precipitation, the particles break off and are

carried for runoff downstream in areas of low depression such as the Aghien lagoon (Dao et al. 2021). Increased rainfall and land use changes could increase the rate of soil erosion in the Aghien Lagoon watershed (Maurya et al. 2021). In this area, soils have been formed on soft materials such as marl and clay, which are not very permeable or impermeable, which favors runoff and soil erosion (Khemiri and Jebari, 2021). Also, the LS factor is an essential factor of the erosive potential (Meliho et al. 2020). Slopes are related to lithology, soil losses become more important with the length and steepness of slopes (Almaaitah et al. 2018). In the study area, the steepest slopes are generally located on the slopes of streams and adjacent valleys (Tsegaye and Bharti, 2021) in the watershed of Aghien lagoon. However, the high and very high soil losses are really insignificant 0.95% (2016) and 0.65% (2020) in the Aghien lagoon watershed, this drop in soil losses in 2020 could be due to the increase in the area of crops/fallow land from 33.92% in 2016 to 41.15%, an increase of 17.56%. However, most of the soil loss in the watershed is due to moderate erosion, which accounts for 1712.19 ha (4.69%) and 1305.77 ha (3.58%) in 2016 and 2020 respectively (Table 14). But also, a drop in this category is observed in 2020. On the other hand, soil losses in the very low (71.49% in 2016 and 77.38% in 2020) to low (22.87% in 2016 and 18.29% in 2020) category are scattered over the watershed. These low values are mainly observed on plateaus, plains, low slopes or almost zero, but also the low soil losses would be linked to the presence of a significant vegetation cover composed of crops and fallow land. This vegetation cover would reduce the velocity of rain drops and favor infiltration in the area (Dawa and Arjune, 2021) by considerably reducing the detachment of soil particles as well as runoff. However, a slight increase in the very low class was observed in 2020, this would be related to the increase in bare soil / Habitats due to the extension of the Autonomous District of Abidjan, despite a lower rainfall than in 2016 (Figure 3) and a fairly high vegetation cover in 2020 (41.15%) than in 2016 (33.92%) (Table 8). According to Nut et al, 2021, bare soil can contribute to increased soil losses in a watershed. However, a contrast is seen when we look at the themes of factor C. This factor reveals that bare soil has increased from 2016 (13.39%) and (21.76%) in 2020, naturally bare soil could favor soil losses, but in this study, these areas are less contributory, as they are located on plateau or low slope areas. This factor reveals that bare soil increases for 2981 ha (37.80%) during 2016-2020, naturally bare soil could favor soil losses, but in this study, these areas are less contributory, as they are located on plateau or low slope areas. The average soil loss values estimated for the watershed over the study period are 60.65% in 2016 and 47.64% in 2020. A regression of the value is contacted in 2020. Nevertheless, the average soil losses are higher than the values found by Nut et al. (2021) on the Stung

Sangkae watershed in Colombia (3.1 and 7.6 t/ha/year in 2002 and 20015 respectively); Sbai et al. (2021) (13.5 t/ha/year) on the Moulouya watershed in eastern Morocco;] Tsegaye and Bharti, (2021) (17.3 t/ha/year) on the Anjed watershed in northwest Ethiopia.

Conclusion

Knowledge of soil erosion requires a quantitative assessment of potential soil erosion. In this study, an empirical USLE model incorporated in the GIS was used to predict the average annual soil erosion in order to estimate the intensity of soil erosion and to preserve soil and natural resources in a watershed of the Aghien Lagoon. The high soil losses are located on the slopes of the rivers and valleys adjacent to the Aghien lagoon, which are also naturally favored by the steepness of the slopes and their length and inclination. However, the average soil loss values are 60.65% in 2016 and 47.64% in 2020. However, the very low and low soil loss values are scattered over the watershed for an area of 34441.52 ha corresponding to a rate of 94.36% in 2016, in 2020 they occupy an area of 34956.76 ha with a rate of 95.77%. On the other hand, high and very high soil losses are insignificant corresponding to rates of 0.95% and 0.60% in 2016 and 2020 respectively. However, most of the soil loss in the watershed is due to moderate erosion, occupying areas of 1712.19 ha (4.69%) and 1305.77 ha (3.58%) also in 2016 and 2020. The evolution of the vegetation cover has had either a negative or positive impact on soil loss in the Aghien lagoon watershed. However, bare soil / Habitats increased from 33.92% in 2016 to 41.15% in 2020.

Acknowledgments

Our thanks go to the “Debt Reduction and Development Contract” (C2D) between France and Côte d’Ivoire which funded the research activities of “Aghien lagoon” project through the partnership PReSeD-CI. This partnership was a very good collaboration between researchers from Université Nangui Abrogoua (UNA), in particular those from the “Laboratoire de Géosciences et Environnement” (LGE) and researchers from the French Institute for Research and Development (IRD).

Conflict of Interest: The authors reported no conflict of interest.

Data Availability: All data are included in the content of the paper.

Funding Statement: The authors did not obtain any funding for this research.

References:

1. Abé, J., N'doufou, G. H. C., Konan, K. E., Yao, K. S., Bamba, S. B., 2014. Relations entre les points critiques d'érosion et le transit littoral en Côte d'Ivoire. Africa Geoscience Review. 21(1-2). 1-14.
2. Adopo, K. L., Akobe, A. C., Etche, M., Monde, S., Aka, K., 2014. Situation de l'érosion Côtière au Sud-est de la Côte d'Ivoire. entre Abidjan et Assinie. Revue Ivoirienne de Science et Technologie. 24. 223-237.
3. Aké, G. É., Kouadio, B. H., Adja, M. G., Ettien, J. B., Effebi K. R., Biémi, J., 2012. Cartographie de la vulnérabilité multifactorielle à l'érosion hydrique des sols de la région de Bonoua (Sud-Est de la Côte d'Ivoire). *Physio-Géo. Géographie physique et environnement.* (Volume 6). 1-42. https://doi.org/10.4000/physio-geo.2285
4. Almaaitah, R., Azhari, A., Asri, R., 2018. Spatial Distribution Of Soil Erosion Risk Using Rusle, Rs And Gis Techniques. *International Journal of Civil Engineering and Technology*, 9(10), 681-697. http://www.iaeme.com/IJCIET/index.as
5. Anache, J. A. A., Bacchi, C. G. V., Panachuki, E., Sobrinho T. A., 2016. Assessment of methods for predicting soil erodibility in soil loss modeling. Geociências (São Paulo), 34(1), 32-40.
6. Batista, P. V. G., Silva, M. L. N., Silva, B. P. C., Curi, N., Bueno, I. T., Júnior, F. W. A., Quinton, J., 2017. Modelling spatially distributed soil losses and sediment yield in the upper Grande River Basin-Brazil. *Catena*, 157, 139-150. http://dx.doi.org/10.1016/j.catena.2017.05.025
7. Belaout, F., Mekerta, B., Zentar, R., Chabani, A., Abdelkrimi, A., Kalloum, S., 2021. Modeling of erosion in the Wadi Guir watershed (South-West Algeria) by the application of Geographic Information System (GIS). International Journal of Forest. Soil and Erosion. 11(1).
8. Benchettouh, A., Kouri, L., Jebari, S., 2017. Spatial estimation of soil erosion risk using RUSLE/GIS techniques and practices conservation suggested for reducing soil erosion in Wadi Mina watershed (northwest. Algeria). *Arabian Journal of Geosciences*. 10(4). 79. http://dx.doi.org/10.5772/intechopen.96190
9. Biswas, S. S., Pani, P., 2015. Estimation of soil erosion using RUSLE and GIS techniques: a case study of Barakar River basin, Jharkhand, India. Modeling Earth Systems and Environment, 1(4), 1-13. DOI 10.1007/s40808-015-0040-3
10. Bollinne, A., Laurant, A., 1983. La prévision de l'érosion en Europe Atlantique : le cas de la zone limoneuse de Belgique. Pédologie, XXXIII, 2, 117-136pp.

11. Bollinne, A., Rosseau P., 1978. Erodibilité des sols de moyenne et haute Belgique. Utilisation d'une méthode de calcul du facteur K de l'équation universelle de perte en terre. Bull. Soc. Géogr. de Liège, 14,4 : 127-140pp.
12. Bouguerra, H., Bouanani, A., Khanchoul, K., Derdous, O., Tachi, S. E., 2017. Mapping erosion prone areas in the Bouhamdane watershed (Algeria) using the Revised Universal Soil Loss Equation through GIS. Journal of water and land development. 32(1). 13-23pp.
13. Boukheir, R., Cerdo, O., Abdallah, C., 2006. Regional soil erosion risk mapping in Lebanon. The Journal of Geomorphology. Vol. 82. Iss. 3 p. 347–359.
14. Coulibaly, L. K., Guan, Q., Assoma, T. V., Fan, X., Coulibaly, N., 2021. Coupling linear spectral unmixing and RUSLE2 to model soil erosion in the Boubo coastal watershed, Côte d'Ivoire. *Ecological Indicators*, 130, 108092. https://doi.org/10.1016/j.ecolind.2021.108092
15. Dao, A., Koffi, E. S., Noufé, D. D., Kamagaté, B., Goné, L. D., Séguis, L., Perrin, J. L., 2021. Soil loss vulnerability: the case study of Aghien lagoon watershed outskirts Abidjan city (Côte d'Ivoire). *Proceedings of the International Association of Hydrological Sciences*, 384, 121-126. https://doi.org/10.5194/piahs-384-121-2021
16. Das, B., Bordoloi, R., Thungon, L. T., Paul, A., Pandey, K. P., Mishra, M., Tripathi O. P., 2020. An integrated approach of GIS. RUSLE and AHP to model soil erosion in West Kameng watershed. Arunachal Pradesh. J. *Earth Syst. Sci.* (2020) 129:94. https://doi.org/10.1007/s12040-020-1356-6
17. Dawa, D., Arjune, V., 2021. Identifying Potential Erosion-Prone Areas in the Indian Himalayan Region Using the Revised Universal Soil Loss Equation (RUSLE). *Asian Journal of Water, Environment and Pollution*, 18(1), 15-23. DOI : 10.3233/AJW210003
18. Déguy, J. P. A., N'Go, A. Y., Kouassi, H. K., Soro, E. G., Goula, A. T. B., 2018. Contribution of a Geographical Information System to the Study of Soil Loss Dynamics in the Lobo Catchment (Côte d'Ivoire). *Journal of Geoscience and Environment Protection*. 6(09). 183. doi: 10.4236/gep.2018.69014.
19. Desmet, P. J. J., & Govers, G. (1996). A GIS procedure for automatically calculating the USLE LS factor on topographically complex landscape units. *Journal of soil and water conservation*, *51*(5), 427-433.
20. Eblin, S. G., Yao, A. B., Anoh, K. A., Soro, N., 2017. Cartographie de la vulnérabilité multifactorielle aux risques d'érosion hydrique des

sols de la région d'Adiaké. sud-est Côtier de la côte d'ivoire. *Revue Internationale des Sciences et Technologie*. 30. 197-216.

21. EL Garouani, A., Chen, H., Lewis, L., Tribak, A., Abharour, M., 2008. Cartographie de l'utilisation du sol et de l'érosion nette à partir d'images satellitaires et du SIG IDRISI au nord-est du Maroc. Télédétection. Editions scientifiques GB. 8 (3), 193-201 pp.
22. Ganasri, B. P., Ramesh, H., 2016. Assessment of Soil Erosion by RUSLE Model Using Rmote Sensing and GIS – A Case Study of Nethravathi. *Basin Geoscience Frontiers*, 7:953-961. https://doi.org/10.1016/j.gsf.2015.10.007
23. Kayet, N., Pathak, K., Chakrabarty, A., Sahoo, S., 2018. Evaluation of soil loss estimation using the RUSLE model and SCS-CN method in hillslope mining areas. International Soil and Water Conservation Research, 6(1), 31-42. https://doi.org/10.1016/j.iswcr.2017.11.002
24. Karydas, C. G., Sekuloska, T., Silleos, G. N. (2009). Quantification and site-specification of the support practice factor when mapping soil erosion risk associated with olive plantations in the Mediterranean island of Crete. *Environmental Monitoring and Assessment*, 149, 19-28. https://doi.org/10.1007/s10661-008-0179-8
25. Khanchoula, K., Selmi, K., Benmarce, K., 2020. Assessment of soil erosion by RUSLE model in the Mellegue watershed, northeast of Algeria. *Environment and Ecosystem Science* (EES), 4(1), 15-22. http://doi.org/10.26480/ees.01.2020.15.22
26. Khemiri, K., Jebari, S., 2021. Évaluation de l'érosion hydrique dans des bassins versants de la zone semi-aride tunisienne avec les modèles RUSLE et MUSLE couplés à un Système d'information géographique. *Cah. Agric*. 30: 7. https://doi.org/10.1051/cagri/2020048
27. Kilic, O. M., 2021. Effects of land use and land cover changes on soil erosion in semi-arid regions of Turkey; a case study in Almus Lake watershed. *Carpathian Journal of Earth and Environmental Sciences*, 16(1), 129-138. DOI: 10.26471/cjees/2021/016/161
28. Kinnell, P. I. A., 2016. A review of the design and operation of runoff and soil loss plots. Catena 145 (2016) 257-265. 10.1016/j.catena.2016.06.013. http://dx.doi.org/10.1016/j.catena.2016.06.013
29. Koffi, E. S., Koffi, K. J. T., Perrin, J-L., Séguis, L., Guilliod, M., Goné, D. L., Kamagaté, B., 2019. Hydrological and water quality assessment of the Aghien Lagoon hydrosystem (Abidjan. Côte d'Ivoire). *Hydrological Sciences Journal*, 64:15. 1893-1908. https://doi.org/10.1080/02626667.2019.1672875

30. Koffi, K. J. P., N'Go, Y. A., Yéo K. M., Koné. D., Savané I., 2014. Détermination des périmètres de protection de la lagune Aghien par le calcul du temps de transfert de l'eau jusqu' à la lagune. *Larhyss Journal* 2 19. 19–3.
31. Koua, J. J. T., Anoh, A. K., Soro, D. T., Kouamé, J. K., Jourda, R. J. P., 2019. Evaluation of Agricultural Practices Scenarios for Reducing Erosion in Buyo Lake Catchment (Sassandra; Côte d'Ivoire) by Use of GIS. *Journal of Geoscience and Environment Protection*. 7(7). 154-171. https://doi.org/10.4236/gep.2019.77011
32. Kouadio, B. H., Kouamé, K. F., Saley, B. M., Biémi, J., 2007. Traoré Ibrahima1Insécurité climatique et géorisques en Côte d'Ivoire : étude du risque d'érosion hydrique des sols dans la région semi-montagneuse de Man (Ouest de la Côte d'Ivoire). Sécheresse vol. 18. n° 1 : 29-37.
33. Kouadio, Z. A., 2018. Spatial Analysis of Erosive Runoff in the Mé Watershed (Côte d'Ivoire). Journal of Water Science and Environment Technologies. 3(02). 376-382.
34. Kouassi, K. H., Koua, T. J. J., Zro, B. G. F., N'Go, Y. A., 2020. Contribution of a Geographical Information System to the study of soil erosion by water in the watershed of the hydro-agricultural dam of Babadou (Côte d'Ivoire). International Journal of Innovation and Applied Studies. 28(2). 458-467.
35. Koukougnon, W. G., Brou, K. M., Silué, Y., Della André, A. L. L. A., 2021. Korhogo à l'épreuve de l'érosion et ses conséquences (nord-Côte d'Ivoire). International Journal of Humanities and Cultural Studies (IJHCS) ISSN 2356-5926. 8(2). 37-50.
36. Markhi, A., Laftouhi ,N-E., Soulaimani, A. Fniguire, F., 2015. Quantification et évaluation de l'érosion hydrique en utilisant le modèle RUSLE et déposition intégrée dans un SIG. Application dans le bassin versant n'fis dans le haut atlas de Marrakech (Maroc). European Scientific Journal, edition vol.11. No.29 ISSN: 1857-7881pp.
37. Maurya, S., Srivastava, P. K., Yaduvanshi, A., Anand, A., Petropoulos, G. P., Zhuo, L., Mall R. K., 2021. Soil erosion in future scenario using CMIP5 models and earth observation datasets. *Journal of Hydrology*, 594, 125851. https://doi.org/10.1016/j.jhydrol.2020.125851
38. Mazouzi, K., El-Hmaidi, A., Bouabid, R., El-Faleh, E-M., 2021. Quantification de l'érosion hydrique par la méthode RUSLE au niveau du bassin versant de l'Oued Mikkès en amont du barrage Sidi Chahed (région de Meknès. Maroc). *European Scientific Journal*, ESJ. 17(14). 256. https://doi.org/10.19044/esj.2021.v17n14p256

39. Meliho, M., Khattabi, A., Mhammdi, N., 2020. Spatial assessment of soil erosion risk by integrating remote sensing and GIS techniques: a case of Tensift watershed in Morocco. *Environmental Earth Sciences*, 79(10), 1-19. https://doi.org/10.1007/s12665-020-08955-y
40. Meliho, M., Khattabi, A., Mhammdi, N., Zhang, H., 2016. Cartographie des risques de l'erosion hydrique par l'Equation Universelle Revisee des Pertes en Sols, la teledetection et les SIG dans le bassin versant de l'ourika (Haut Atlas, Maroc), *Eur. Scient. J.*, 12, 32, https://doi.org/10.19044/esj.2016.v12n32p277
41. N'Dri, W. K. C., Pistre, S., Jourda ,J. P., Kouamé, K. J., 2021. Application of a Deterministic Distributed Hydrological Model for Estimating Impact of Climate Change on Water Resources in Côte d'Ivoire Using RCP 4.5 and RCP 8.5 Scenarios: Case of the Aghien Lagoon. Dr. Mustafa Turkmen; Dr. Kwong Fai Andrew Lo. International Research in Environment, Geography and Earth Science Vol. 9, 9, Book Publisher International (a part of SCIENCEDOMAIN International), pp.129 - 153, 2021, 978-93-91215-91-0. ff10.9734/bpi/ireges/v9/5512dff. ffhal-03254861f
42. Nana, P. P., 2018. Du groupe à l'individu : dynamique de la gestion foncière en pays gouin (sud-ouest du Burkina Faso), Belgeo URL http://journals,openedition,org/belgeo/21653 6080; https://doi.org/10.4000/belgeo.26080
43. N'Dri, B. É., Niamké, K. H., Koudou, A., N'Go, Y. A., 2017. Cartographie des formes d'érosion hydrique dans la commune urbaine d'attécoubé (Abidjan. Côte d'Ivoire) /mapping of water erosion forms in the urban district of Attecoube (Abidjan. Côte d'Ivoire). International Journal of Innovation and Applied Studies. 19(4). 960.
44. Nut, N., Mihara, M., Jeong, J., Ngo, B., Sigua, G., Prasad, P. V., Reyes, M. R., 2021. Land use and land cover changes and its impact on soil erosion in Stung Sangkae catchment of Cambodia. *Sustainability*, 13(16), 9276. https://doi.org/10.3390/su13169276
45. Onyando, J O., Kisoyan, P., Chemelil, M. C., 2005. Estimation of potential soil erosion for river Perkerra catchment in Kenya; *Water Resour. Manag*. 19(2) 133–143. https://doi.org/10.1007/s11269-005-2706-5
46. Panagos, P., Borrelli, P., Meusburger, K., Alewell, C., Lugato, E., Montanarella, L., 2015a. Estimating the soil erosion cover-management factor at the European scale. Land use policy, 48, 38-50. http://dx.doi.org/10.1016/j.landusepol.2015.05.021
47. Panagos, P., Borrelli, P., Poesen, J., Ballabio, C., Lugato, E., Meusburger, K., Alewell, C., 2015b. The new assessment of soil loss

by water erosion in Europe. Environmental science and policy, 54, 438-447. https://doi.org/10.1016/j.envsci.2015.08.012

48. Payet, E., Dumas, P., Pennober, G., 2012. Modélisation de l'érosion hydrique des sols sur un bassin versant du sud-ouest de Madagascar, le Fiherenana. VertigO: la revue électronique en sciences de l'environnement, 11(3). https://id.erudit.org/iderudit/1015047ar
49. Piyathilake, I. D. U. H., Sumudumali, R. G. I., Udayakumara, E. P. N., Ranaweera, L. V., Jayawardana, J. M. C. K., Gunatilake, S. K., 2021. Modeling predictive assessment of soil erosion related hazards at the Uva province in Sri Lanka. Modeling Earth Systems and Environment, 7(3), 1947-1962. . https://doi.org/10.1007/s40808-020-00944-1
50. Renard, K. G., Freimund, J. R., 1994. Using monthly precipitation data to estimate the R-factor in the revised USLE. Journal of hydrology, 157(1-4), 287-306.
51. Renard, K. G., Foster, G. R., Weesies, G. A., McCool, D. K., Yoder, D. C., 1996. Predicting soil erosion by water: A guide to conservation planning with the Revised Universal Soil Loss Equation (RUSLE). Agriculture handbook, 703, 25-28.
52. Roose, E. J., Lelong, F., 1976. Les facteurs de l'érosion hydrique en Afrique Tropicale. Études sur petites parcelles expérimentales de sol. Revue de géographie physique et de géologie dynamique. Vol. 18. Iss. 4 p. 365–374.
53. Roose, E. J., 1977. Use of the Universal Soil Loss Equation to Predict Erosion in West Africa. In Soil erosion: Prediction and control. Soil Conservation Society of America, Special Publication no. 21. Ankeny, Iowa.
54. Rougerie, G., 1958. Modalité du ruissellement sous forêt dense de Côte d'Ivoire. CR Acad Sci Paris ; 246 : 290-2.
55. Rougerie, G., 1960. Le façonnement actuel des modelés en Côte d'Ivoire forestière. Mémoire IFAN 58. Dakar : Institut Fondamental d'Afrique Noire (IFAN).
56. Sbai, A., Mouadili, O., Hlal, M., Benrbia, K., Zahra Mazari, F., Bouabdallah, M., Saidi, A., 2021. Water Erosion in the Moulouya Watershed and its Impact on Dams' Siltation (Eastern Morocco). Proceedings of the International Association of Hydrological Sciences, 384, 127-131.
57. Songu, G. A., Abu, R. D., Temwa, N. M., Yiye S. T., Wahab, S., Mohammed, B. G., 2021. Analysis of Soil Erodibility Factor for Hydrologic Processes in Kereke Watershed, North Central Nigeria. *Journal of Applied Sciences and Environmental Management*, 25(3), 425-432. https://dx.doi.org/10.4314/jasem.v25i3.18

58. Stone, R. P., Hilborn, D., 2000. Universal Soil Loss Equation-Factsheet. http://www.omafra.gov.on.ca/english/engineer/facts/00-001.htm
59. Swarnkar, S., Malini, A., Tripathi, S., Sinha, R., 2018. Assessment of uncertainties in soil erosion and sediment yield estimates at ungauged basins: an application to the Garra River basin, India. *Hydrology and Earth System Sciences*, 22(4), 2471-2485. https://doi.org/10.5194/hess-22-2471-2018
60. Tian, Y. C., Zhou, Y. M., Wu, B. F., & Zhou, W. F. (2009). Risk assessment of water soil erosion in upper basin of Miyun Reservoir, Beijing, China. *Environmental Geology*, *57*, 937-942. https://doi.org/10.1007/s00254-008-1376-z
61. Toumi, S., Meddi, M., Mahé, G., Brou, Y-T., 2013. Cartographie de l'érosion dans le bassin versant de l'Oued Mina en Algérie par télédétection et SIG. *Hydrological Sciences Journal,* l58. 01- 17. https://doi.org/10.1080/02626667.2013.824088.
62. Traoré, A., Soro, G., Kouadio, E. K., Bamba, B. S., Oga, M. S., Soro, N., Biémi, J., 2012. Evaluation des paramètres physiques. chimiques et bactériologiques des eaux d'une lagune tropicale en période d'étiage : la lagune Aghien (Côte d'Ivoire). *International Journal of Biological and Chemical Sciences*. 6(6). 7048-7058. http://dx.doi.org/10.4314/ijbcs.v6i6.40
63. Trimble., 2010. eCognition® Developer 8.64.0 Reference Book. (Available at: http://www.definiens.com/ . Access on may 11, 2015)
64. Tsegaye, L., Bharti, R., 2021. Soil erosion and sediment yield assessment using RUSLE and GIS-based approach in Anjeb watershed, Northwest Ethiopia. *SN Applied Sciences*, 3(5), 1-19. https://doi.org/10.1007/s42452-021-04564-x
65. Vrieling, A., 2005. Satellite remote sensing for water erosion assessment. a review. CATENA. Vol. 65. Iss. 1 p. 2–18
66. Wachal, D. J., Banks, K. E., Hudak, P. F., Harmel, R. D., 2009. Modeling erosion and sediment control practices with RUSLE 2.0 : A management approach for natural gas well sites in Denton County. TX. USA. *Environmental geology*. 56(8). 1615-1627pp. https://doi.org/10.1007/s00254-008-1259-3
67. Wischmeier, V. H., Smith, D. D., 1978. Predicting rainfall erosion losses- a guide to conservation planning. United States Department of Agriculture in cooperation with Purdue Agricultural Experiment Station. United States Department of Agriculture. Washington. Agriculture Handbook No. 282.

68. Zhou, P., Luukkanen, O., Tokola, T., Nieminen, J., 2008. EAect of vegetation cover on soil erosion in a mountainous watershed; *Catena* 75(3) 319–325pp. https://doi.org/10.1016/j.catena.2008.07.010